



Published in final edited form as:

*Genesis*. 2019 January ; 57(1): e23259. doi:10.1002/dvg.23259.

## Using human sequencing to guide craniofacial research

Ryan P. Liegel<sup>1,a</sup>, Erin Finnerty<sup>1</sup>, Lauren Blizzard<sup>1</sup>, Andrew DiStasio<sup>1</sup>, Robert B. Hufnagel<sup>1,b</sup>, Howard M. Saal<sup>1,4</sup>, Kristen L. Sund<sup>1,4</sup>, Cynthia A. Prows<sup>1,2,4</sup>, Rolf W. Stottmann<sup>1,3,4</sup>

<sup>1</sup>Division of Human Genetics, Cincinnati Children's Hospital Medical Center, University of Cincinnati College of Medicine, Cincinnati, Ohio 45229

<sup>2</sup>Division of Patient Services, Cincinnati Children's Hospital Medical Center, University of Cincinnati College of Medicine, Cincinnati, Ohio 45229

<sup>3</sup>Division of Developmental Biology, Cincinnati Children's Hospital Medical Center, University of Cincinnati College of Medicine, Cincinnati, Ohio 45229

<sup>4</sup>Department of Pediatrics, Cincinnati Children's Hospital Medical Center, University of Cincinnati College of Medicine, Cincinnati, Ohio 45229

### Summary

A recent convergence of technological innovations has re-energized the ability to apply genetics to research in human craniofacial development. Next-generation exome and whole genome sequencing have significantly dropped in price, making it relatively trivial to sequence and analyze patients and families with congenital craniofacial anomalies. A concurrent revolution in genome editing with the use of the CRISPR-Cas9 system enables the rapid generation of animal models, including mouse, which can precisely recapitulate human variants. Here, we summarize the choices currently available to the research community. We illustrate this approach with the study of a family with a novel craniofacial syndrome with dominant inheritance pattern. The genomic analysis suggested a causal variant in *AMOTL1* which we modeled in mice. We also made a novel deletion allele of *Amotl1*. Our results indicate that *Amotl1* is not required in the mouse for survival to weaning. Mice carrying the variant identified in the human sequencing studies, however, do not survive to weaning in normal ratios. The cause of death is not understood for these mice complicating our conclusions about the pathogenicity in the index patient. Thus, we highlight some of the powerful opportunities and confounding factors confronting current craniofacial genetic research.

### Keywords

birth defects; mammal; organism; process; genetics; process; organogenesis; process; neural crest; tissue; other; tissue

---

**Correspondence** Rolf Stottmann, Division of Human Genetics, Cincinnati Children's Hospital Medical Center, University of Cincinnati College of Medicine, Cincinnati, OH 45229. rolf.stottmann@cchmc.org.

<sup>a</sup>Present address: Morgridge Institute for Research, University of Wisconsin, Madison, WI.

<sup>b</sup>Present address: National Eye Institute, National Institutes of Health, 10 Center Drive, Building 10, Room 10N109, Bethesda, MD 20892.

## 1 | INTRODUCTION

During the first trimester of human development, multiple tissue prominences are created which then grow and fuse to form the early elements of the face. Proper formation of the craniofacial tissues requires coordination of multiple cell types of different embryonic origins to ultimately produce the morphologically complex mature craniofacial structures. A particularly critical cell type for craniofacial development is the neural crest cell (NCC) population. NCCs are born at the interface of the neural and surface ectoderm and migrate to multiple positions in the body and contribute to the majority of the craniofacial structures. Disruption of proper craniofacial development leads to craniofacial anomalies which are some of the most common congenital anomalies with a collective incidence of approximately 1/600 live births (Shaw, 2004). These anomalies are typically divided into two main classifications: isolated cleft lip and/or cleft palate or, alternatively, syndromic malformations where additional tissues are affected. A caveat to these classifications is, of course, that the undiscovered phenotypes in any specific patient may or may not be related to a specific variant causing the craniofacial anomaly originally called an isolated cleft, especially given all the lineages NCCs contribute to.

The genetic basis of craniofacial development and congenital malformations has been an area of investigation since the earliest understandings of heredity. Many genetic requirements for specific genes were elucidated by targeted loss of function experiments in multiple model organisms. Other genes have been identified by large scale mutagenesis forward genetic screens, or even spontaneous mutations in animal colonies. An increasingly effective approach is to directly apply next-generation sequencing efforts to affected humans and their biologic family members. The rapid advances in technology make sequencing ever more accessible, even to laboratory groups not traditionally considered to be human geneticists. The long-heralded “\$1,000 genome” in which the entire human genome can be sequenced at sufficient depth for robust analysis is now readily available on a research basis.

The primary challenge then is not the identification of variant(s) which may contribute to a congenital craniofacial anomaly but, rather, assigning pathogenicity to a specific variant. One could attempt to do this by collecting multiple families with very similar phenotypic features and look for variants held in common across affected individuals from many families to identify variants that are not just shared by descent. This approach is, however, completely dependent on clinicians with phenotyping expertise to identify multiple families with key features, the difficulty of which is directly proportional to the rarity of the phenotype in the population. An alternative approach is to identify candidate variants within a family. While a trio approach with an affected proband and unaffected parents is most commonly used, phenotypes that seem to be segregating in a dominant fashion may require two trios as distantly related as possible within a family unless an affected family member with an apparent de novo variant is available.

A parallel approach is to generate a biological model of a suspected variant to truly demonstrate pathogenicity. This is tremendously facilitated by the recent advances in genome editing in both cellular and animal models. This approach will then also create an experimental substrate to understand the underlying molecular mechanism(s) and even

potentially test therapeutic intervention strategies. A number of experimental options confront the researcher tasked with this challenge. Cellular models can be derived directly from the patients as fibroblasts or used in conjunction with cellular reprogramming techniques to create induced Pluripotent Stem Cells (iPSCs). iPSCs can then be used to create many different cell types. Isogenic iPSC lines can be made to rescue or recreate suspected pathogenic variants and test how the lines differ in experimental settings (Fatehullah, Tan, & Barker, 2016). Embryological models include frog, chick, and zebrafish. The relative merits of these have been extensively reviewed elsewhere (Van Otterloo, Williams, & Artinger, 2016). Larger animal models can also be created including goats, pigs, and monkeys with CRISPR-Cas9 editing (Cui et al., 2018; Hai, Teng, Guo, Li, & Zhou, 2014; Ni et al., 2014). We favor the mouse models for a combination of accessible genetics, relative cost, fast generation time, and physical resemblance to human biology as compared to many other genetic models. (We, of course, acknowledge that no animal model is a true recapitulation of human biology and for some genes, the causative mutation simply does not function similarly in any nonhuman model.) Here, we illustrate both the power of this approach and some of the difficulties in modeling suspected human pathogenic variants in the mouse. We have used next-generation sequencing on a multigenerational family including two members with craniofacial anomalies. This analysis identified a compelling novel variant we suspected to be pathogenic. We then chose to model this variant and create a novel null allele of this gene in the mouse to test this prediction.

## 2 | RESULTS

### 2.1 | Whole exome sequencing of a family with a novel craniofacial syndrome

The proband was the 4.0 kg, 50.8 cm product of a 39 week gestation to a 39-year-old Gravida 1, Para 0–1 woman and her 29-year-old unrelated partner. Maternal gestational diabetes was noted at 8 weeks gestation but well controlled with insulin. The proband was born with a complete left sided cleft lip with cleft palate and right sided cleft of the primary palate. Prenatal fetal echocardiogram demonstrated a ventricular septal defect (VSD) in addition to the cleft lip with cleft palate. Postnatal echocardiogram showed a VSD with tetralogy of Fallot and a double orifice mitral valve. Neurologic examination was unremarkable. The early childhood clinical course was complicated by obstructive sleep apnea secondary to short mandible with glossoptosis. A large cisterna magna was incidentally identified during an airway Magnetic Resonance Imaging (MRI) scan and has remained stable in subsequent imaging. At 14 years of age, advanced bone age (2.1 standard deviation) was incidentally identified during hand films to evaluate the proband's concerns about bent fingers.

The family history was significant as the proband's father was also born with a left-sided unilateral complete cleft lip and cleft palate. He also had an atrial septal defect (ASD) repaired in early childhood and a reported mitral valve abnormality. Similar to the proband, the father was tall in stature and had large dysplastic ears. The proband has no biologic siblings and there is no other family history of cleft lip, cleft palate, or congenital heart defects.

At age 11 years, the proband, affected father, unaffected mother, and unaffected paternal grandparents were enrolled in an institutionally funded investigational whole exome sequencing project for undiagnosed disorders (Figure 1a). Alignment and variant detection were performed using the Broad Institute's web-based Genome Analysis Toolkit (GATK; Genome Reference Consortium Build 37). The Golden Helix SNP and Variation suite (Bozeman, MT) was used for data filtering of VCF files containing a combined total of 107,135 variants. After quality control, 95,228 remaining variants were filtered for variants which were (a) *de novo*; (b) coding and nonsynonymous; and (c) found only in the biologic father and transmitted to the proband. A single missense variant in *angiomin like 1* (*AMOTL1*) 11:94532825, c.469C>T; p.Arg157Cys met all these criteria and presumably arose spontaneously in the father and was transmitted to the proband. The variant is in a region of the AMOTL1 protein which is highly conserved through many vertebrate species including chicken and frog (Figure 1b). This variant is absent from the ExAC and gnomAD database at the time of writing; is considered "deleterious" by Sorting Intolerant From Tolerant (SIFT), "disease causing" by MutationTaster and "probably damaging" by PolyPhen-2; and the amino acid physiochemical difference is considered large with a Grantham score of 180 (0–215). An independent analysis of the sequence was run with Ingenuity Variant Analysis (Qiagen), replicated the finding in the father and proband but also identified an AMOTL1 missense variant c.712C>T, rs201051216, p.Arg238Cys (MAF < 0.001 in NHLBI ESP6500, European Americans, 15 heterozygotes in ExAC) in the healthy mother that was transmitted to the son. Both AMOTL1 variants were confirmed with Sanger sequencing in the proband and transmitting parents (Figure 1c and data not shown). Further analysis focused on the unique paternal *de novo* c.469C>T variant because father and proband share key congenital anomalies and the other missense variant identified in the unaffected mother is seen in control populations.

## 2.2 | Novel mouse alleles of *Amotl1*

We took advantage of the ability to quickly make targeted mutations in the mouse with CRISPR-Cas9 genome editing and constructed an allelic series of *Amotl1* with the goal of disrupting gene function and also recapitulating the R157C variant at the orthologous amino acid position in the mouse genome. *Amotl1* had not been deleted in the mouse at the time of experimental design. We chose to keep and maintain two alleles from the CRISPR-Cas9 founder mice. *Amotl1<sup>em1Rstot</sup>* (*Amotl1<sup>R157C</sup>*) is the arginine to cysteine coding change identified in the human exome analysis. We also recovered a one base pair deletion *Amotl1<sup>em2Rstot</sup>* (*Amotl1<sup>D1</sup>*) resulting in a reading frameshift that produces a protein with 15 nonsensical amino acids after position 155 and a premature stop codon (Figure 2). We also recovered an eight base pair deletion *Amotl1<sup>em3Rstot</sup>* (*Amotl1<sup>D8</sup>*) resulting in a reading frameshift that produces a protein with 34 nonsensical amino acids after position 153 and a premature stop codon.

We bred each of these alleles to test for viability (Table 1). We first noted that *Amotl1<sup>R157C/wt</sup>* heterozygotes did not survive in Mendelian ratios at weaning, as approximately one-third of the expected animals were not recovered. Surviving *Amotl1<sup>R157C/wt</sup>* heterozygotes were intercrossed and we noted that the number of *Amotl1<sup>R157C/R157C</sup>* homozygotes was substantially reduced at weaning and *Amotl1<sup>R157C/wt</sup>*

heterozygotes were again under-represented from the remaining animals. We examined newborn litters at postnatal day (P)0 and P1 to begin to determine the stage of death and found the homozygotes were slightly under-represented at birth. All four homozygotes we recovered at P0 were already dead within hours of birth. An embryonic analysis from embryonic day (E)13.5–E18.5 showed no loss of *Amotl1<sup>R157C/R157C</sup>* homozygotes or *Amotl1<sup>R157C/wt</sup>* heterozygotes at organogenesis stages. We further show that this is true when the data are subdivided into early organogenesis (E13.5–E15.5) and later organogenesis stages (E16.5–E18.5; Table 1). We thus conclude that the *Amotl1<sup>R157C</sup>* leads to incompletely penetrant lethality at perinatal stages. We next examined the survival of the *Amotl1<sup>D1</sup>* deletion and found that animals homozygous for the *Amotl1<sup>D1</sup>* deletion were viable and fertile as homozygotes with no significant deviation from Mendelian expectations. We found similar results with the *Amotl1<sup>D8</sup>* deletion and did not pursue this allele further.

The craniofacial and cardiac phenotypes in the human patients with the *AMOTL1<sup>R157C</sup>* variant both suggest mechanisms that might account for perinatal lethality in the mouse. We therefore examined the *Amotl1<sup>R157C</sup>* mice for these phenotypes. We did not see any evidence of cleft palate in 24 *Amotl1<sup>R157C/wt</sup>* embryos at E16.5–E18.5 and in 10 P0 *Amotl1<sup>R157C/wt</sup>* pups. We also examined 9 *Amotl1<sup>R157C/R157C</sup>* embryos at these stages and did not see signs of cleft palate in these animals either (Figure 3a,b). Skeletal preparations, gross examinations and micro-computed tomography (micro-CT) imaging studies were performed but did not reveal any phenotypes to explain the perinatal lethality in either *Amotl1<sup>R157C/wt</sup>* or *Amotl1<sup>R157C/R157C</sup>* embryos (Figure 3c,f). We also examined *Amotl1<sup>R157C/wt</sup>* and *Amotl1<sup>R157C/R157C</sup>* embryos for structural heart defects with a combination of whole mount and/or histological analysis with a special attention for septal and valve defects and outflow tract anomalies. Analysis of at least 16 *Amotl1<sup>R157C/wt</sup>* and 6 *Amotl1<sup>R157C/R157C</sup>* embryos at E16.5–E18.5 showed no evidence of outflow tract defects, septal defects or valvular anomalies. We also examined multiple *Amotl1<sup>R157C/wt</sup>* mice at P28 and saw no evidence for heart phenotypes at this age either (Figure 4).

The expression of a missense variant may lead to an unstable protein, so we overexpressed in vivo a myc-tagged AMOTL1 protein as well as a modified construct to recapitulate the *AMOTL1<sup>R157C</sup>* patient variant. Overexpression in HEK293T cells showed that the variant protein is produced by the cell but the AMOTL1-R157C-myc variant is not found on control protein (Figure 5a). We attempted to assay the runs as a larger protein species on the gel suggesting a post-levels of AMOTL1 protein in *Amotl1<sup>D1/D1</sup>* mutant embryos. We were, translational modification may be present on the variant protein which however, unable to unambiguously detect AMOTL1 expression in vivo in a number of tissues where *Amotl1* expression is reported. Thus, we cannot definitively address the effects of these mutations on AMOTL1 levels in vivo but suspect the *Amotl1<sup>D1</sup>* allele to be a loss of function or severely hypomorphic allele based on the amino acid sequence change. As the *Amotl1<sup>D1</sup>* deletion creates a premature stop, we asked if the transcript for that variant was degraded by nonsense-mediated decay (He & Jacobson, 2015) and prepared cDNA from control and homozygous mutant embryos. While there is a trend toward a reduction in mRNA levels in mutant tissues as compared to wild-type, it does not reach statistical significance (Figure 5b,c).

### 3 | DISCUSSION

Here, we illustrate one strategy to assess pathogenicity of variants identified in sequencing of a family with an inherited craniofacial anomaly. Exome sequencing of five members of the family suggested one de novo variant in *AMOTL1* may be the causal genetic lesion. Based on our preference for the mouse as the experimental model, we used CRISPR-Cas9 genome editing techniques to recreate the human variant and test the hypothesis this is the cause of the congenital anomaly. As a germline deletion of *Amotl1* has not been published to our knowledge, we took advantage of the possibility to also recover insertion/ deletion alleles from the transgenic founders. We conclude that *Amotl1* is not absolutely required in the mouse for survival to adulthood in a standard vivarium environment. We further show that the *Amotl1*<sup>R157C</sup> missense variant identified in the human genetics studies significantly reduces viability of mice.

*Amotl1* is a member of the motin family of genes comprised of *angiomin*, *angiomin-like 1* (*Amotl1*) and *angiomin-like 2* (*Amotl2*; Bratt et al., 2002). Mice lacking *angiomin* die around E11.5 with vascular defects (Aase et al., 2007). Motin family members have been shown to interact with Wnt and Hippo signaling (Chan et al., 2011; Li et al., 2012; Paramasivam, Sarkeshik, Yates 3rd, Fernandes, & McCollum, 2011; Ragni et al., 2017), but no germline deletion of *Amotl1* has been reported. Consistent with our conclusions, we do note that the international mouse phenotyping consortium ([mousephenotype.org](http://mousephenotype.org)) has produced a gene trap allele of *Amotl1* and do not report any phenotypes in a thorough array of tests from 13 homozygous *Amotl1*<sup>tm1a(EUCOMM)Wtsi</sup> mutants (Koscielny et al., 2014). This may be because of functional compensation by other members of the *Amotl* gene family.

The interpretation of the data from the *Amotl1*<sup>R157C</sup> allele is a bit more difficult. It is clear that the mutation compromises survival of the mouse and is probably acting as a dominant allele with incomplete penetrance. We were unable to determine the mechanism of death. The most obvious candidate systems based on time of death and the human proband phenotypes were craniofacial and cardiovascular development. However, we were not able to detect phenotypes in these tissues consistent with a perinatal lethality phenotype. We hypothesize that the *Amotl1*<sup>R157C</sup> allele is a neomorphic allele which acts in a dominant negative fashion. We are not able then to definitively address the hypothesis that the *Amotl1*<sup>R157C</sup> variant identified is related to the human pathology. We suspect that the human patients represent the more mild effects of a *AMOTL1*<sup>R157C</sup> variant. Although we did not find comparable phenotypes between the human patients and mice, we do find it hard to believe we created the precisely same variant leading to a dominant effect on survival at random. However, as none of the phenotypes match between the human patients and mouse models, we are unable to make strong conclusions. These findings of underrepresented *Amotl1*<sup>R157C</sup> mice in our colony could formally be the result of “off-target” CRISPR-Cas9 editing at an independent locus which than actually is the cause of the lethality. The most recent litters we have reported here are four and five generations removed from the CRISPR founders. A nonlinked mutation would thus have a 6% and 3% chance, respectively (0.5<sup>4</sup>, 0.5<sup>5</sup>), to be inherited and causal. Of the top 11 predicted off-target sites for the guide sequence used in the construction of the allele, only one is on chromosome 9. This

sequence is 88 Mb and 50 cM away from *Amot11* so is essentially totally unlinked with *Amot11*. In addition, we specifically kept the two deletion lines, *Amot11<sup>D1</sup>* and *Amot11<sup>D8</sup>*, as complementary data sets to support our conclusions.

This study illustrates a few aspects of studies using animal models to assess human genetic findings. Next generation sequencing is now quite readily applicable to the study of human congenital malformations. This study was initiated a few years ago and utilized an exome sequencing approach focused on just the coding region of the genome. As sequencing technologies have evolved, unbiased whole genome sequencing is now becoming cost effective. Moreover, as the genome sequencing approach does not require the selective hybridization of the exonic sequences and avoids some of the biases from this library capture, the whole genome sequencing approach has been shown to generate more even coverage of the exome (Meienberg, Bruggmann, Oexle, & Matyas, 2016). We are now pursuing similar approaches to that described here in other families by directly employing whole genome sequencing at surprisingly affordable rates. We do, however, acknowledge that the genomics community is currently challenged to interpret the vast majority of noncoding variants that come out of a whole genome analysis. However, the data generated by this approach will remain a constant for each patient (with the caveat of acquired mosaic mutations), is easily stored, and can be periodically reanalyzed as our genomic understanding and capacity increases.

The amount of data in a whole genome sequencing experiment is immense but is relatively easy to manage in the context of rare congenital malformation studies. A crucial point of the experimental design is to include as many family members as practical and feasible in the analysis. The proband and parents (trio) are a normal minimum, but any siblings (affected or unaffected) and extended family can be useful as well. This additional information allows for significant filtering and exclusion of identified variants. In the case of the family presented here, a dominant inheritance model was assumed. Thus, any variants not exclusive to the proband and his father can be eliminated in a first pass analysis. Another powerful tool is the ever-increasing number of genomes of control populations being deposited into public databases. This is especially true for the structural birth defects community. The genome aggregation database ([gnomAD.broadinstitute.org](http://gnomAD.broadinstitute.org)) is one such resource and at the time of this writing has 123,136 exome sequences and 15,496 whole genome sequences (Lek et al., 2016). Other such efforts are also being made around the world. These projects allow us to begin to define the range of “normal” genetic variation in the adult human population. The individuals in the gnomAD project are known to not have severe pediatric disease. This method of collection means that in a first pass analysis of the results, any variant found with a minor allele frequency of greater than 1% or 0.1% in both the control databases and an affected individual can be initially classified as not causal. An even more aggressive strategy can potentially be applied where the presence of the allele in a control population to any degree suggests it may not be causal. Incomplete penetrance is, of course, a major caveat to this, but the first task in a genome analysis is to remove variants until a manageable number can be manually curated to formulate hypotheses. Datasets can always be reanalyzed with relaxed filters and constraints as necessary.

Recent complementary technologies make this a tremendously exciting time to be performing this kind of work with a wealth of tools at the disposal of the structural birth defect and craniofacial genetics research community. Animal models have been a valued experimental approach for a number of years but the advent of CRISPR-Cas9 mediated genome editing techniques means that conserved genes can be manipulated in model organisms to precisely model human variants. If the candidate gene in question has not previously been studied, the mechanics of CRISPR-Cas9 editing allow us to readily make an allelic series to create putative null alleles in the same experiment as the variant modeling. This is a fundamentally different approach than previous homologous recombination-based methodologies carried out in embryonic stem cells used to make chimeric founder animals. A potential challenge to this approach (especially relevant for craniofacial biology) is the modeling of a dominant negative allele with perinatal lethal phenotypes. Modern medical care often allows humans with congenital craniofacial anomalies to thrive with surgical intervention. In the absence of such modalities, the laboratory mouse will die from many craniofacial anomalies preventing the researcher from establishing a stable transgenic line. An alternative approach is to perform the CRISPR-Cas9 genome edits *in vitro* and, rather than let these animals be born to breed out the mutation, recover those treated embryos directly from the surrogate dam (an “F0 CRISPR” approach). A phenotypic and genomic analysis of these embryos can be performed to address hypotheses about genetic variants.

Conclusions about pathogenicity are much more convincing when the phenotypes of the animal model match the human model (DiStasio et al., 2017). These models then offer an experimental platform for detailed analysis of embryonic molecular mechanism as well as a tool to test any therapeutic interventions that can be devised. Cases such as the one we report here represent examples where the interpretation is much more difficult and almost certainly cannot result in a clinically significant return of results to the family. The fact that the identical variant identified in exome analysis recapitulated in the mouse model results in unexplained lethality in mice suggests there clearly is some molecular pathogenesis. However, it is likely unwise to use this finding to direct clinical care. Rather, these represent tantalizing insights into structural birth defects biology that warrant further experimental effort.

## 4 | METHODS

### 4.1 | Patient sequencing and variant confirmation

Informed consent/assent was obtained from all subjects according to Cincinnati Children’s Hospital Medical Center (CCHMC) institutional review board protocol #2012–0203. All methods and experimental protocols were carried out in accordance with relevant guidelines and regulations and with approval from the CCHMC Institutional Biosafety Committee. Following consent, whole blood was collected. Library generation, exome enrichment, sequencing, alignment, and variant detection were performed in the CCHMC Genetic Variation and Gene Discovery Core Facility (Cincinnati, OH). Briefly, sheared genomic DNA was enriched with NimbleGen EZ Exome V2 kit (Madison, WI). The exome library was sequenced using Illumina’s Hi Seq 2000 (San Diego, CA). Alignment and variant



detection was performed using the Broad Institute's web-based GATK (McKenna et al., 2010). All analyses were performed using Genome Reference Consortium Build 37.

#### 4.2 | Variant filtering and pathogenicity assessment

Quality control and data filtering were performed on VCF files in Golden Helix's SNP and Variation Suite (Bozeman, MT) as well as Ingenuity Variant Analysis (Qiagen, Germany). Nonsynonymous coding variants were compared to three control databases, including NHLBI's ESP6500 exome data (Fu et al., 2013), the 1,000 genomes project (Genomes Project et al., 2010), EXAC Browser (Karczewski et al., 2017), and an internal CCHMC control cohort (Patel et al., 2014). The identified variant was compared to known disease genes in the OMIM and Human Gene Mutation (Stenson et al., 2014) databases, and to reported variants in dbSNP (Sherry et al., 2001) and the Exome Variant Server. The variant was also analyzed using Interactive Biosoftware's Alamut v2.2 (San Diego, CA) to determine location of mutation within a protein domain, the conservation of the amino acid, the Grantham score (Grantham, 1974) and the designation of the mutation by three existing in silico software tools, SIFT (Li, Gui, Kwan, Bao, & Sham, 2012), Polyphen (Adzhubei et al., 2010), and Mutation Taster (Schwarz, Rodelsperger, Schuelke, & Seelow, 2010).

#### 4.3 | Mouse allele generation

CRISPR guides for *Amot1l* were evaluated using the Fusi ([Benchling.com](http://Benchling.com)) and Moreno-Mateos ([Crisprscan.org](http://Crisprscan.org)) algorithms. Potential guide RNA (gRNA) sequences were selected and ordered as complementary oligonucleotide pairs with BbsI over-hangs (Integrated DNA Technologies (IDT), Coralville, IA). These were ligated into the pSpCas9(BB)2A-GFP (px458) vector and transfected into MK4 cells at low confluence using the Lipofectamine 2000 transfection reagent (Thermo Fisher Scientific, MA). Cells were harvested 48 hr after transfection and genomic DNA was isolated and used with the Surveyor mutation detection kit (IDT) in order to test gRNA cutting efficiency. As a control, cutting efficiencies of potential guides were compared with that of a previously published mTet2 gRNA. Cas9 and gRNAs were injected into C57BL/6N zygotes (Taconic) by the CCHMC Transgenic Core. Potential founders were validated with Sanger sequencing of tail DNA and subsequently maintained on a C57BL/6J (Jackson Labs) background. pSpCas9(BB)-2 A-GFP (PX458) was a gift from Feng Zhang (Addgene plasmid #48138). All alleles are available to the research community upon publication. PCR primers and sequences along with CRISPR donor oligo sequence are shown in Table 2.

#### 4.4 | Animal husbandry

All animals were housed under an approved protocol in standard conditions. All euthanasia and subsequent embryo or organ harvests were preceded by Isoflurane sedation. Euthanasia was accomplished via dislocation of the cervical vertebrae. For embryo collections, noon of the day of vaginal plug detection was designated as E0.5.

#### 4.5 | Histological analysis

Tissue samples were fixed in Bouin's fixative solution. Samples were then paraffin embedded, sectioned at 6  $\mu$ m for adult tissue and 10  $\mu$ m for embryonic tissue, and

processed through hematoxylin and eosin (H&E) or Nissl staining. Sections were sealed using Cytoseal Mounting Medium (Thermo Fisher Scientific). All paired images are shown at the same magnification.

#### 4.6 | *Amotl1* overexpression and cDNA analysis

An *Amotl1* expression construction encoding an AMOTL1-myc fusion protein tag was purchased from Origene (#RC207693, Rockville, MD). Site directed mutagenesis to recreate the R157C variants was performed with QuikChange Lightning Site-Directed Mutagenesis kit (Agilent, Santa Clara, CA). HEK293T cells were transfected with standard protocols. Western immunoblotting was performed with standard protocols and a primary polyclonal rabbit antibody (PA5-42267 from ThermoFisher). RNA was extracted and purified from *Amotl1<sup>D1</sup>* animals and wild-type controls with TRIZOL reagent. cDNA was prepared with Superscript III reverse transcriptase and random hexamer primers. qRT-PCR was performed with FAM labeled, TaqMan gene expression probes (Thermo Fisher) for *Amotl1* (Mm01171515) and *Gapdh* (Mm99999915) on an Applied Biosystems 7300 Real Time PCR System.  $C_t$  values were calculated in relation to a standard curve over a 5-log RNA dilution series as a ratio of *Amotl1* to *Gapdh* (average of three replicates for each).

Measurements from patient records were converted to metric system units with an on-line tool ([www.metric-conversions.org](http://www.metric-conversions.org)).

## ACKNOWLEDGMENTS

We are grateful to Yueh-Chiang Hu and the CCHMC Transgenic Animal and Genome Editing Core for advice and technical assistance, and to Katherine Yutzey for extensive discussion of the cardiovascular analysis prior to publication. Funding for this study was provided by the Cincinnati Children's Research Foundation and the CCHMC Center for Pediatric Genomics.

Funding information

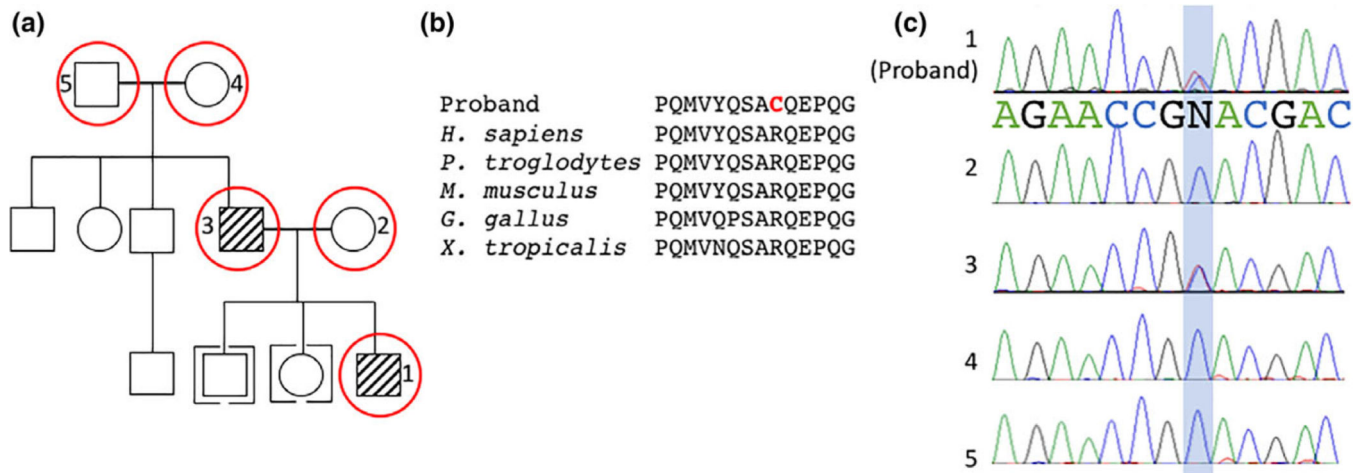
Cincinnati Children's Research Foundation; CCHMC Center for Pediatric Genomics

## REFERENCES

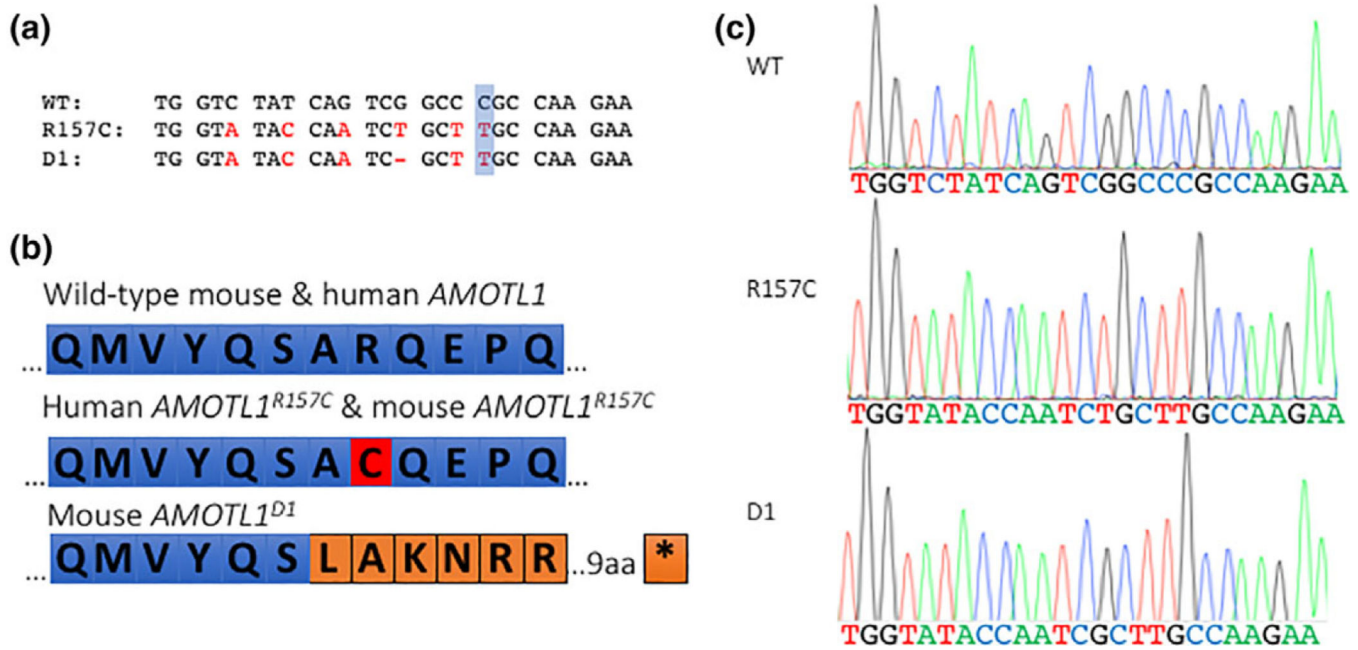
- Aase K, Ernkvist M, Ebarasi L, Jakobsson L, Majumdar A, Yi C, ... Holmgren L. (2007). Angiotonin regulates endothelial cell migration during embryonic angiogenesis. *Genes & Development*, 21, 2055–2068. [PubMed: 17699752]
- Adzhubei IA, Schmidt S, Peshkin L, Ramensky VE, Gerasimova A, Bork P, ... Sunyaev SR (2010). A method and server for predicting damaging missense mutations. *Nature Methods*, 7, 248–249. [PubMed: 20354512]
- Bratt A, Wilson WJ, Troyanovsky B, Aase K, Kessler R, Van Meir EG, & Holmgren L. (2002). Angiotonin belongs to a novel protein family with conserved coiled-coil and PDZ binding domains. *Gene*, 298, 69–77. [PubMed: 12406577]
- Chan SW, Lim CJ, Chong YF, Pobbati AV, Huang C, & Hong W. (2011). Hippo pathway-independent restriction of TAZ and YAP by angiotonin. *The Journal of Biological Chemistry*, 286, 7018–7026. [PubMed: 21224387]
- Cui Y, Niu Y, Zhou J, Chen Y, Cheng Y, Li S, ... Ji W. (2018). Generation of a precise Oct4-hrGFP knockin cynomolgus monkey model via CRISPR/Cas9-assisted homologous recombination. *Cell Research*, 28, 383–386. [PubMed: 29327727]

- DiStasio A, Driver A, Sund K, Donlin M, Muraleedharan RM, Pooya S, ... Stottmann RW (2017). *Copb2* is essential for embryogenesis and hypomorphic mutations cause human microcephaly. *Human Molecular Genetics*, 26, 4836–4848. [PubMed: 29036432]
- Fatehullah A, Tan SH, & Barker N. (2016). Organoids as an in vitro model of human development and disease. *Nature Cell Biology*, 18, 246–254. [PubMed: 26911908]
- Fu W, O'Connor TD, Jun G, Kang HM, Abecasis G, Leal SM, ... Akey JM (2013). NHLBI Exome Sequencing Project; Analysis of 6,515 exomes reveals the recent origin of most human protein-coding variants. *Nature*, 493, 216–220. [PubMed: 23201682]
- Genomes Project C, Abecasis GR, Altshuler D, Auton A, Brooks LD, Durbin RM, ... McVean GA (2010). A map of human genome variation from population-scale sequencing. *Nature*, 467, 1061–1073. [PubMed: 20981092]
- Grantham R. (1974). Amino acid difference formula to help explain protein evolution. *Science*, 185, 862–864. [PubMed: 4843792]
- Hai T, Teng F, Guo R, Li W, & Zhou Q. (2014). One-step generation of knockout pigs by zygote injection of CRISPR/Cas system. *Cell Research*, 24, 372–375. [PubMed: 24481528]
- He F, & Jacobson A. (2015). Nonsense-mediated mRNA decay: Degradation of defective transcripts is only part of the story. *Annual Review of Genetics*, 49, 339–366.
- Karczewski KJ, Weisburd B, Thomas B, Solomonson M, Ruderfer DM, Kavanagh D, ... MacArthur DG (2017). The ExAC browser: Displaying reference data information from over 60,000 exomes. *Nucleic Acids Research*, 45, D840–D845. [PubMed: 27899611]
- Koscielny G, Yaikhom G, Iyer V, Meehan TF, Morgan H, AtienzaHerrero J, ... Parkinson H. (2014). The international mouse Phenotyping consortium web portal, a unified point of access for knockout mice and related phenotyping data. *Nucleic Acids Research*, 42, D802–D809. [PubMed: 24194600]
- Lek M, Karczewski KJ, Minikel EV, Samocha KE, Banks E, Fennell T, ... Exome Aggregation Consortium. (2016). Analysis of protein-coding genetic variation in 60,706 humans. *Nature*, 536, 285–291. [PubMed: 27535533]
- Li MX, Gui HS, Kwan JS, Bao SY, & Sham PC (2012). A comprehensive framework for prioritizing variants in exome sequencing studies of Mendelian diseases. *Nucleic Acids Research*, 40, e53. [PubMed: 22241780]
- Li Z, Wang Y, Zhang M, Xu P, Huang H, Wu D, & Meng A. (2012). The *Amotl2* gene inhibits Wnt/beta-catenin signaling and regulates embryonic development in zebrafish. *The Journal of Biological Chemistry*, 287, 13005–13015. [PubMed: 22362771]
- McKenna A, Hanna M, Banks E, Sivachenko A, Cibulskis K, Kernytzky A, ... DePristo MA (2010). The genome analysis toolkit: A MapReduce framework for analyzing next-generation DNA sequencing data. *Genome Research*, 20, 1297–1303. [PubMed: 20644199]
- Meienberg J, Bruggmann R, Oexle K, & Matyas G. (2016). Clinical sequencing: Is WGS the better WES? *Human Genetics*, 135, 359–362. [PubMed: 26742503]
- Ni W, Qiao J, Hu S, Zhao X, Regouski M, Yang M, ... Chen C. (2014). Efficient gene knockout in goats using CRISPR/Cas9 system. *PLoS ONE*, 9, e106718.
- Paramasivam M, Sarkeshik A, Yates JR 3rd, Fernandes MJ, & McCollum D. (2011). Angiomotin family proteins are novel activators of the LATS2 kinase tumor suppressor. *Molecular Biology of the Cell*, 22, 3725–3733. [PubMed: 21832154]
- Patel ZH, Kottyan LC, Lazaro S, Williams MS, Ledbetter DH, Tromp H, ... Kaufman KM (2014). The struggle to find reliable results in exome sequencing data: Filtering out Mendelian errors. *Frontiers in Genetics*, 5, 16. [PubMed: 24575121]
- Ragni CV, Diguët N, Le Garrec JF, Novotova M, Resende TP, Pop S, ... Meilhac SM (2017). *Amotl1* mediates sequestration of the hippo effector Yap1 downstream of Fat4 to restrict heart growth. *Nature Communications*, 8, 14582.
- Schwarz JM, Rodelsperger C, Schuelke M, & Seelow D. (2010). MutationTaster evaluates disease-causing potential of sequence alterations. *Nature Methods*, 7, 575–576. [PubMed: 20676075]
- Sherry ST, Ward MH, Kholodov M, Baker J, Phan L, Smigielski EM, & Sirotkin K. (2001). dbSNP: The NCBI database of genetic variation. *Nucleic Acids Research*, 29, 308–311. [PubMed: 11125122]

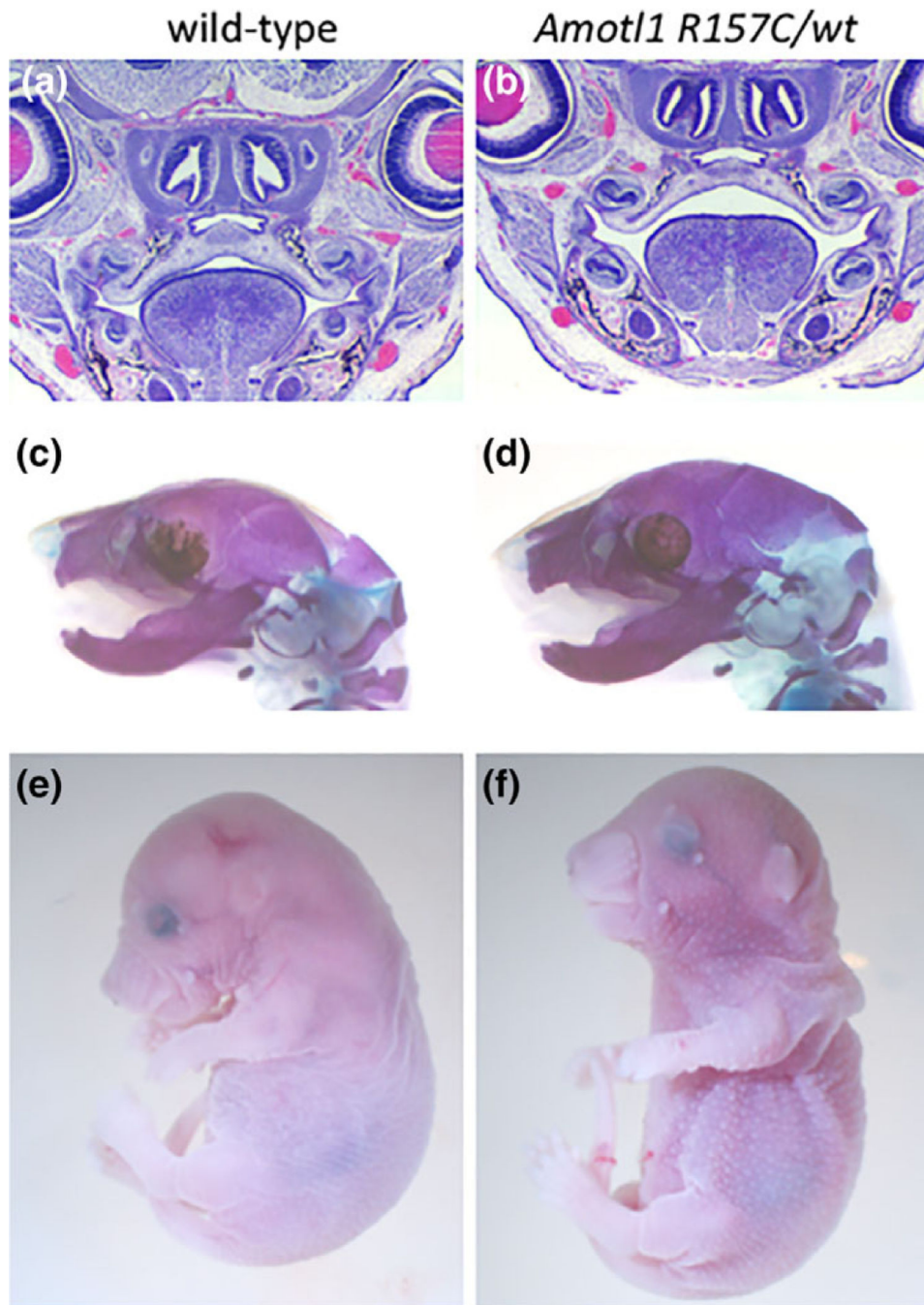
- Stenson PD, Mort M, Ball EV, Shaw K, Phillips A, & Cooper DN (2014). The human gene mutation database: Building a comprehensive mutation repository for clinical and molecular genetics, diagnostic testing and personalized genomic medicine. *Human Genetics*, 133, 1–9. [PubMed: 24077912]
- Shaw W. (2004). Global strategies to reduce the health care burden of craniofacial anomalies: Report of WHO meetings on international collaborative research on craniofacial anomalies. *The Cleft PalateCraniofacial Journal*, 41, 238–243.
- Van Otterloo E, Williams T, & Artinger KB (2016). The old and new face of craniofacial research: How animal models inform human craniofacial genetic and clinical data. *Developmental Biology*, 415, 171–187. [PubMed: 26808208]

**FIGURE 1.**

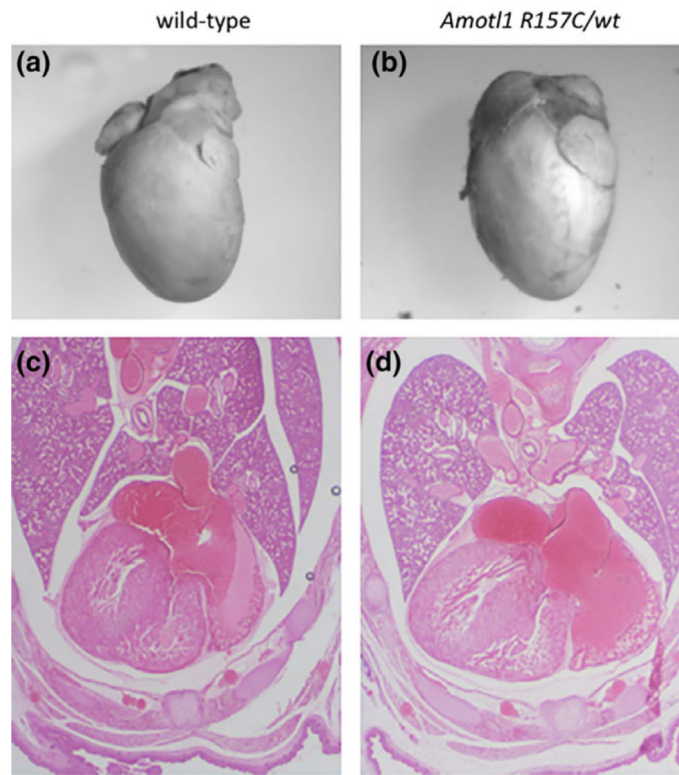
A novel congenital malformation syndrome. (a) Pedigree of proband (patient 1). Affected members are shown with the hash marks and the circled members were selected for exome sequencing. (b) The variant in *AMOTL1* affects as highly conserved arginine residue. (c) Sanger sequencing of indicated family members confirms the *AMOTL1* sequence variant is present in only patients 1 and 3

**FIGURE 2.**

An allelic series of *Amotl1* in the mouse. (a) Wild-type nucleotide sequence of *Amotl1* around the desired single nucleotide C>T mutation (blue shaded box). Sequence analysis of *Amotl1*<sup>R157C</sup> mice in this region indicates the desired genome edit was made along with other silent mutations (shown in red) to facilitate CRISPR guide stability and genotyping of modified mice. *Amotl1*<sup>D1</sup> sequence is shown: (–) indicates the deleted nucleotide. (b) The predicted proteins for wild-type and each of the genome edits. The R157C variant is a single missense codon (red), while the D1 deletion changes codon usage to create 15 missense amino acids (orange) before a stop codon. (c) Sanger sequence validation of the sequence results schematized in (b)

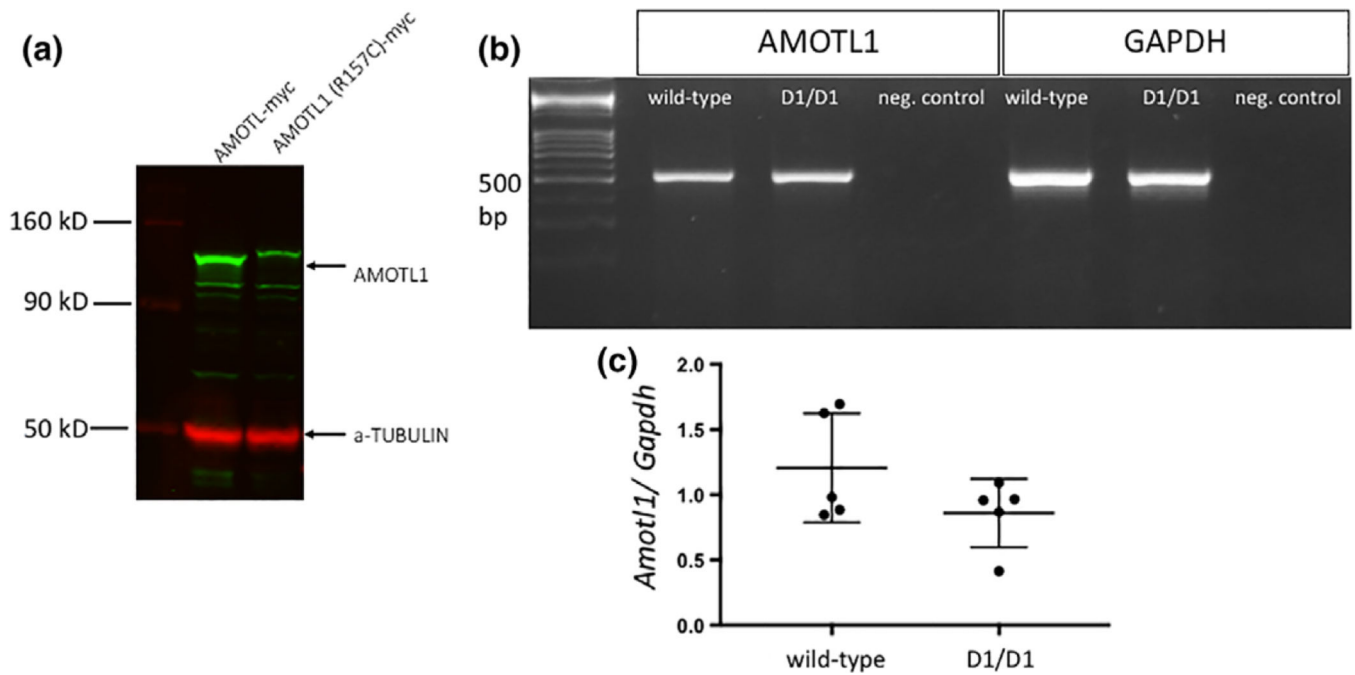


**FIGURE 3.** Mice carrying the *Amotl1*<sup>R157C</sup> variant are healthy and fertile. Histological analysis (a, b), skeletal preparations (c, d) and whole mount analysis (e, f) do not reveal any phenotypes which allow us to explain the perinatal lethality in *Amotl1*<sup>R157C/wt</sup> mice as compared to wild-type



**FIGURE 4.** Cardiac development is normal in *Amot1*<sup>R157C</sup> mice. Whole mount and histological analysis indicates cardiac development is relatively unaffected in *Amot1*<sup>R157C/wt</sup> mice



**FIGURE 5.**

*Amotl1* variants do not significantly affect protein or mRNA levels. (a) Overexpression of *AMOTL1*<sup>R157C</sup>-myc indicates the coding change may allow a post-translational modification which changes the apparent size of the protein. Over a series of experiments, we do not notice a consistent and significant change in protein levels. (b) cDNA RT-PCR analysis shows that the premature stop codon in the *Amotl1*<sup>D1</sup> allele does not trigger nonsense-mediated decay. Gapdh is shown as a control reaction. (c) Quantitative RT-PCR of five wild-type and five mutant RNA samples from E14.5 head tissue run in triplicate shows no significant reduction in *Amotl1* mRNA levels. Data are shown with the mean and upper/lower 95% confidence interval of the mean indicated with horizontal bars

TABLE 1

Survival of mice with targeted *AMOTL1* alleles

	Wild-type	Heterozygous	Homozygous	Chi <sup>2</sup>
<i>Amotl1</i> R157C × wt	44 (35)	25 (35)	N/A	0.022
<i>Amotl1</i> R157C intercross	89 (54)	113 (107)	12 (54)	6.63E-13
<i>Amotl1</i> R157C (P0, P1)	14 (6)	7 (12)	4 <sup>a</sup> (6)	0.056
<i>Amotl1</i> R157C (E13.5–E18.5)	29 (24)	47 (48)	22 (24)	0.55
<i>Amotl1</i> R157C (E13.5–E15.5)	11 (9)	17 (18)	8 (9)	0.73
<i>Amotl1</i> R157C (E16.5–E18.5)	18 (16)	30 (31)	15 (16)	0.74
<i>Amotl1</i> D1 intercross	30 (25)	47 (50)	24 (25)	0.54
<i>Amotl1</i> D8 intercross	26 (18)	30 (36)	15 (18)	0.078

Note. Expectations for normal Mendelian ratios are shown parenthetically.

<sup>a</sup> All R157C homozygotes recovered at P0 were dead upon discovery.

TABLE 2

PCR primers	
<i>AMOTL1</i> exon3 F	GGTAAATGGAGGTGATGATGC
<i>AMOTL1</i> exon3 R	CTGCTTCAGTTCCCTTCAGCG
<i>AMOTL1</i> exon3 F (nested with above)	TGTGGAGCTGCCTGATATCTT
<i>AMOTL1</i> exon3 R (nested with above)	CTTATGGCCTGTCCACTGT
mAmotl1 exon 3.1F (intronic)	AGAACAGAGGCCCCAGGAAGTCT
mAmotl1 exon 3.1R	GAGCTCCTCGTTGTTCTGCTGAG
mAmotl1 exon 3.2F	ACAAATGGTCTATCAGTCGGCC
mAmotl1 exon 3.2R	AGACAGGCTGAGCTGGGGATG
<i>Amotl1</i> CRISPR guide sequence	TCCACAAATGGTCTATCAGT
<i>Amotl1</i> R157C CRISPR donor oligo	CTGCTTCTCCATCACCGTATTGTCTCCCTGATGCTCTTGAC CTGCGGTTCTTGGCAAAGCAGATGGTATACCAATTTGTGGATC TTCTTTGAGTGAGGGTTCCCGTGGAGAAAAGTTGGT
<i>Amotl1</i> cDNA F	GTCCCATGATCGCCCCAT
<i>Amotl1</i> cDNA R	CTGCTTCTCCATCACCGTATTG
Gapdh cDNA F	CTTTGGCATTTGTGGAAGGG
Gapdh cDNA R	CCTCTCTTGGCTGCAGTGTC